Optical tunneling of single-cycle terahertz bandwidth pulses

M. T. Reiten, D. Grischkowsky, and R. A. Cheville
School of Electrical and Computer Engineering and Center for Laser and Photonics Research, Oklahoma State University, Stillwater, Oklahoma 74078

(Received 7 March 2001; published 27 August 2001)

We report time-domain measurements with subpicosecond resolution of optical tunneling of terahertz electromagnetic pulses undergoing frustrated total internal reflection. Measurements of the transmitted electromagnetic pulses over a 3 THz bandwidth permits direct determination of frequency-dependent phase and amplitude changes in both the thin and opaque barrier limits in a single measurement. A complex frequency response function describing propagation through the barrier is developed based upon linear dispersion theory and the Fresnel coefficients at complex angles in the optical barrier. Our measurements are in excellent agreement with this theoretical model across the experimentally determined bandwidth; the model makes no assumptions about the beam path through the barrier and has no adjustable parameters. The theory is shown to satisfy the Kramers-Kronig relations, indicating causal propagation across the barrier.

DOI: 10.1103/PhysRevE.64.036604 PACS number(s): 41.20.Jb, 42.25.−p, 73.40.Gk, 78.47.+p

There has been an ongoing discussion for many years over the question of whether or not light propagates at superluminal velocities during optical tunneling in frustrated total internal reflection (FTIR) in wedges, photonic band gaps, and waveguides below cutoff [1]. Although seemingly of rather esoteric interest, the problem has far-reaching implications such as violations of causality [1], what consists of a signal, and the correct way to define the velocity of energy propagation [2,3]. Additionally, the equations describing FTIR are mathematically similar to the equations describing quantum-mechanical tunneling [4–6], with the optical tunneling of FTIR being used as an experimentally verifiable model for the quantum-mechanical case.

From a practical point of view, FTIR is used in fiber couplers, laser output couplers, and photon tunneling microscopes. Photonic band-gap structures are commonly used in optical devices such as vertical cavity surface emitting lasers and chirped mirrors [7]. The related question of tunneling times for electrons is critical to the fundamental speed limits of existing devices as tunnel diodes and Josephson junctions, as well as resonant tunneling diodes and transistors being investigated for nanoelectronics.

Recent demonstrations [8] of superluminal optical pulse propagation in a gain medium for an extremely narrow bandwidth signal have stimulated a renewed interest in whether signals can propagate faster than the speed of light. In the optical tunneling system investigated here, similar claims [9] of superluminal propagation have been made for wide bandwidth signals. There is a lack of consensus on the definition of energy or signal velocity and what consists of a signal, making it of critical importance to tie experimental observations to precise definitions of the quantity being measured [1]. Many experimental systems have been used to provide insight into optical tunneling at optical [10,11], far-infrared [9], and microwave frequencies [7,12,13]. Optical techniques can measure pulse delays with femtosecond accuracy and have large dynamic range; however, it is difficult to measure absolute optical phase and reliably fabricate structures with nanometer precision. Some of these problems inherent in optical experiments are solved by microwave measurements that permit direct measurement of phase. Most microwave experiments have been done confining radiation to waveguide structures since the large wavelengths require large apertures and large experimental systems to make measurements in the plane-wave limit.

The optical tunneling system investigated here, consisting of an optical barrier in which electromagnetic radiation undergoes total internal reflection, has been looked at previously, both theoretically and experimentally. An excellent review of experimental and theoretical results on tunneling time measurements that include those for this system has been given by Chiao and Steinberg in 1997 [1]. More recent experimental work includes measurement of pulse propagation times using both microwave measurements in paraffin prisms [13] as well as measurements of terahertz pulses in a teflon prism [9].

We report measurements of optical tunneling using terahertz time-domain spectroscopy (THz-TDS) [14] which directly contradict earlier claims of noncausal propagation [9]. In our experiment, the time-resolved electric fields of single-cycle terahertz pulses transmitted through a pair of cylindrical wedges (prisms) are experimentally measured with femtosecond accuracy as a function of tunneling gap, or barrier, thickness. The corresponding phase and amplitude changes are fit to a frequency-domain linear dispersion theory incorporating an absolute optical phase that describes propagation of a plane electromagnetic field through the optical tunneling gap. Previous claims of non-causal propagation [9] were based on the improper assignment of a ray path through the gap. The complete theory developed here determines the absolute phase change of electromagnetic radiation propagating through the entire cylindrical wedge system, independent of specification of the path through the gap. This is the first direct measurement of absolute optical phase change in optical tunneling with sufficient bandwidth to cover both the thin and thick barrier limits in a single measurement. The ability to perform time-resolved electric-field measurements allows a comparison to an analytic, causal theory with excellent agreement in both the time and frequency domains. This

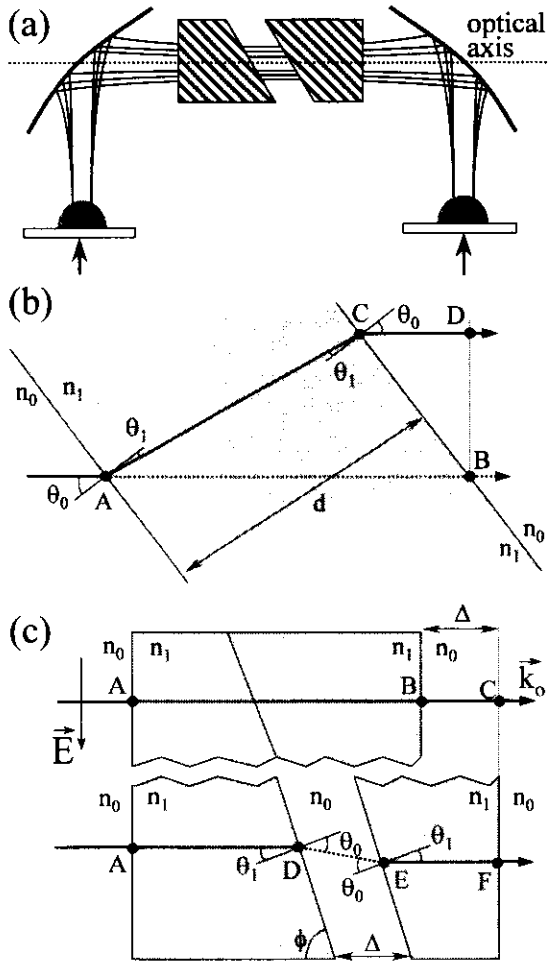

FIG. 1. (a) Terahertz time-domain spectroscopy system used for measuring frustrated total internal reflection. The terahertz beam propagates along the indicated optical axis. (b) Detail of terahertz pulse propagation through a dielectric slab of thickness, d. (c) Terahertz pulse propagation through silicon cylindrical wedges for the reference pulse path (upper) and after translation the second wedge by an amount Δ (lower).

theory fully describes the propagation of a plane wave through the entire optical tunneling barrier system.

The THz-TDS system [14] used to perform FTIR measurements is shown in Fig. 1(a). The generated terahertz radiation forms a well-collimated beam with a gaussian amplitude profile [15] which propagates through two cylindrical wedges used to create the optical tunneling barrier. The matched wedges are of high-resistivity silicon, 75 mm in diameter, optically polished on all faces, shown in Fig. 1(c). High-resistivity silicon was used for wedge materials since it has nearly negligible absorption across the terahertz frequency range [14] with index variations less than 0.02%. The wedges have entrance and exit faces normal to the cylinder axis and inner faces with a vertex angle, $\phi = 70°$. When the wedges are in contact ($\Delta = 0$) they form a 68-mm long cylinder. Both the separation Δ between the wedges along the cylinder axis and the angle of the terahertz system optical axis to the cylinder axis are adjustable with a resolutions of 1 μm and 0.1°, respectively.

The wedges are cut so the beam is incident at an angle of 20°, 3° beyond the critical angle in silicon, $\theta_c = 17.04°$. At the critical angle, the attenuation length of the evanescent wave in the gap has a singularity, and is extremely sensitive to the angle of incidence with 20× variation over a 0.01° range [16]. By increasing the incidence angle beyond θ_c, the attenuation length decreases and becomes much less sensitive to the angle of incidence. Our bounded terahertz beam has a 8.5 mm $1/e$ amplitude waist radius at 0.5 THz, corresponding to a range of incidence angles of the plane-wave components that make up the bounded beam of less than ±0.5° [17]. To minimize the frequency dependence of the k vector uncertainty, the optical system generates a beam waist (planar phase front) at the gap whose radius is proportional to wavelength.

In THz-TDS two time-resolved electric-field measurements are taken, a reference pulse that measures the system response, and the terahertz pulse with a sample in the beam. The reference pulse, $E_O(t)$, was measured with the separation Δ along the cylindrical wedge axes set to zero, shown in the upper portion of Fig. 1(c). Measurements of the transmitted pulse, $E_T(t)$, which optically tunneled through the sample, were made for $\Delta = 100$, 200, 500, and 1000 μm, lower portion of Fig. 1(c). The terahertz pulses were P polarized with detection extinction of over 1000:1 in power. These measurements are shown as points in Fig. 2(a) ($\theta_0 = \pi/2 - \phi = 20°$). The peak of the transmitted terahertz pulse arrives earlier in time with increasing barrier width; the pulse for $\Delta = 1000\,\mu$m arrives 2.4 ps before the reference pulse ($\Delta = 0$). There is strong attenuation of the high-frequency components and pulse reshaping as Δ increases. The frequency-dependent attenuation can be seen from the amplitude spectra, obtained from a numerical Fourier transform of the time-domain data and shown as points in Fig. 2(b). The amplitude spectra have not been scaled; the area under each curve squared is proportional to the transmitted pulse energy. The energy of the pulse transmitted through the 1000 μm gap is approximately 22,000 times smaller than that of the reference pulse.

Optical tunneling of terahertz pulses is analyzed using linear dispersion theory. The Fourier transform of the time-resolved electric-field $E(t)$ gives the complex, frequency-dependent amplitude $E(\omega)$ of the plane-wave components of the terahertz pulse. Each plane-wave component propagates through the optical tunneling barrier, which can be treated as a dielectric slab, shown in Fig. 1(b). The initial standard analysis describes a slab with index n_1 surrounded by a medium with index n_0. These results will then be transformed to the tunneling geometry of a gap with index n_0 surrounded by a medium with index n_1. The field $E_T(\omega)$ transmitted through a dielectric slab is obtained from the superposition of the directly transmitted field with the components that undergo multiple reflections from each interface (see Ref. [18], sections 1.6.4 and 7.6.1):

$$E_T(\omega) = \frac{t_{01}t_{10}e^{i\beta}}{(1 + r_{01}r_{10}e^{i2\beta})} E_I(\omega). \tag{1}$$

The dielectric slab is of thickness d, measured normal to the slab faces, and the radiation is incident at angle θ_0. $E_I(\omega)$ is the incident field. The Fresnel coefficients are t_{01}, t_{10}, r_{01},

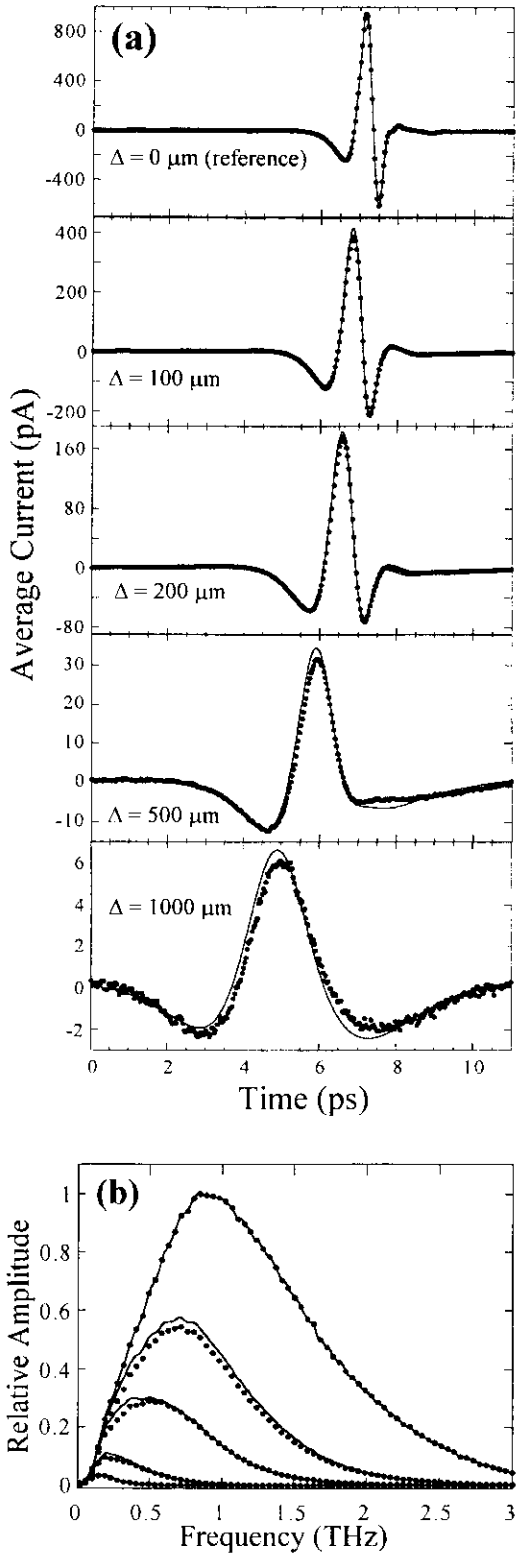

FIG. 2. Measured terahertz pulses (points) propagating through FTIR cylindrical wedges with $\Delta=0$, 100, 200, 500, and 1000 μm. The linear dispersion theory fit is given by the solid line. (b) Measured amplitude spectra (points) corresponding to the terahertz pulses of (a) with theoretical predictions (lines). The amplitude spectra are presented as measured with no scaling.

and r_{10} for transmission and reflection at the n_0-n_1 and n_1-n_0 boundaries, respectively, the subscripts correspond to the dielectric medium. $\beta=n_1 k_o d\cos\theta_1$ is the phase delay associated with multiple reflections inside the slab, with k_o the wave vector in free space. θ_1 is the angle of the transmitted radiation inside the slab determined from Snell's law, $n_0\sin\theta_0=n_1\sin\theta_1$.

Adding such a dielectric slab to the terahertz beam path requires an additional phase term in Eq. (1), which arises from replacing space (n_0) with dielectric ($n_1\neq n_0$). The THz-TDS experiment measures the change in phase between two arbitrary phase fronts, located in front of and behind the slab. The measured phase change is calculated from the optical path length difference between a phase front of the beam in free space and the beam that propagates through the slab measured at the same phase front. Any physically valid measurement must account for the displacement of space by the dielectric slab. Ignoring the effect of the space displaced by the slab is equivalent to measuring the phase at two different spatial points.

This additional phase term will now be evaluated for the dielectric slab illustrated in Fig. 1(b). The input phase front is defined as point A and output phase front is the line BD. The optical path length through free space is $AB=n_0 d/\cos\theta_0$. Defining $E_I(\omega)$ as the incident field at the input plane and $E_O(\omega)$ as the field that propagated through free space, $E_O(\omega)=E_I(\omega)\exp[ik_o l_{AB}]$. Adding a dielectric slab to the beam path changes the optical path, now given by $l_{AC}+l_{CD}=n_1 d/\cos\theta_1+2n_1 d\tan\theta_1\sin\theta_0$. The field that propagates through the dielectric slab is now $E_T(\omega)=E_I(\omega)\exp[ik_o(l_{AC}+l_{CD})]$.

For the dielectric slab $E_O(\omega)$ and $E_T(\omega)$ are experimentally measured; $E_I(\omega)$ would never be directly determined. Expressing the incident field in terms of the measured field transmitted through free space, $E_I(\omega)=E_O(\omega)\exp[-ik_o l_{AB}]$ the measured phase delay of the initial pulse is determined from $E_T(\omega)=E_O(\omega)\exp[ik_o(l_{AC}+l_{CD}-l_{AB})]$ where $k_o(l_{AC}+l_{CD}-l_{AB})=k_o n_1 d\cos\theta_1-k_o n_0 d\cos\theta_0$. This phase delay applies to all terms, including the Fabry-Perot reflections represented by the denominator of Eq. (1). In terms of measured quantities, the field transmitted through the dielectric slab is now given by

$$\mathbf{E}_T(\omega)=\frac{t_{01}t_{10}e^{i\beta}e^{-i\gamma}}{(1+r_{01}r_{10}e^{i2\beta})}E_O(\omega), \tag{2}$$

with $\beta=n_1 k_o d\cos\theta_1$ and $\gamma=k_o n_0 d\cos\theta_0$. The correction factor γ accounts for the displacement of free space with a dielectric material that occurs in any physical measurement. Neglecting the γ term with $n_1>n_0$ results in the nonphysical situation of phase advance as the incident angle θ_0 and optical path length increase.

To treat the cylindrical wedges shown in Fig. 1(c), the wedges with no gap, $\Delta=0$, are taken as a reference. The measured phase difference occurs between the phase front at the input face, point A, and a phase plane corresponding to the output face after the wedges are separated, line CF. The

measured amplitude and phase changes in the terahertz beam are due to two terms. The first arises from the gap DE created by the translation of one wedge that is modeled as a dielectric slab of index n_0 surrounded by a medium with index n_1 with thickness $d=\Delta \sin\phi$, and tilted at angle $\theta_1 = \pi/2-\phi$ relative to the optical axis of the terahertz system. For incident angles below the critical angle, the path through the gap is well defined. The second term $e^{i\Phi}$ arises from the fact that the gap was not achieved by removing silicon from the beam path, but by translation of the second wedge by an amount Δ; the air space BC of index n_0 becomes filled with a medium of index n_1. The transmitted field $E_T(\omega)$ is then given by

$$E_T(\omega)=\frac{t_{10}t_{01}e^{i\beta_0-i\gamma_1}}{(1+r_{10}r_{01}e^{i2\beta_0})}\times e^{i\Phi}\times E_O(\omega)=H(\omega)E_O(\omega). \tag{3}$$

The first term, or phase change due to the gap, has the same form as Eq. (2) with the indices 0 and 1 reversed. Here, $\beta_0 = n_0 k_o d\cos\theta_0$, and the reference path length correction factor is given by $\gamma_1 = n_1 k_o d\cos\theta_1$. The term $\exp[i\Phi]$ gives the phase change between the measured and reference pulses due to the translation of the exit face by Δ with $\Phi = n_1 k_o \Delta - n_0 k_o \Delta$, assuming normal incidence.

For an angle of incidence on the gap greater than critical angle $\theta_1 > \theta_c$, the field in the gap becomes nonuniform, corresponding to creation of an evanescent field with exponentially decreasing amplitude in the gap to satisfy the boundary conditions [18] (Sec. 1.5.4). The ray path DE in the gap is no longer well defined; the optical path does not directly correspond to a phase change since the phase of the transmitted field is independent of z. This uncertainty in the path of the pulses is one reason it has been so difficult to assign a characteristic time for optical tunneling [1].

However, mathematical specification of the path is not required for Eq. (3) to remain valid, as we will now demonstrate. Following Ref. [18] (Sec. 1.5.4), we assume Eq. (3) may still be applied for radiation incident past the critical angle, where the angle θ_0 now becomes complex, $\theta_0 = a + ib$, with real part, $a=\pi/2$, and an imaginary part, $b = \pm\cosh^{-1}(n_1 \sin\theta_1/n_2)$. The sign of b is chosen to avoid the nonphysical situation of energy gain in the gap. The term β_0 in Eq. (3) is now purely imaginary with $\cos(\theta_0) = \pm i[(n_1/n_0)^2\sin^2(\theta_1)-1]^{1/2}$, which rapidly increases from zero at $\theta_1=\theta_c$ to approximately $(n_0/n_1)^{1/2}$ for $\theta_1=90°$. Since $\cos(\theta_0)$ also enters into the Fresnel coefficients—t_{10}, t_{01}, and r_{10}—there is an additional phase change or temporal shift of the radiation propagating through the boundary. Note that in the case that θ_0 is complex, the path of the radiation in the gap is not mathematically defined as when θ_0 is real valued.

The terahertz pulse transmitted through the cylindrical wedges is calculated by taking the inverse Fourier transform of the complex amplitude $E_T(\omega)$ from Eq. (3) with the measured $E_O(\omega)$. The calculated terahertz pulse is plotted as a solid line on top of the data for $\Delta = 100$, 200, 500, and 1000 μm in Fig. 2(a). The calculated amplitude spectra, again given as solid lines, are overlaid on the experimental measurements in Fig. 2(b). Excellent agreement is obtained with no adjustable parameters, indicating the validity of Eq. (3).

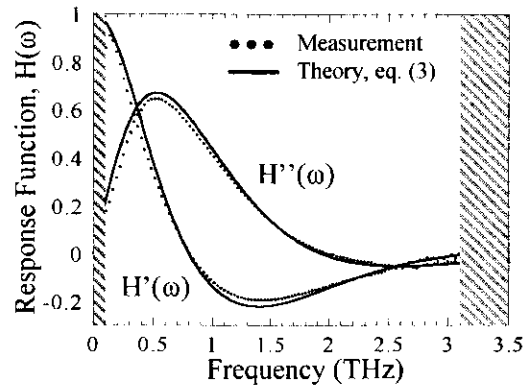

FIG. 3. (a) The measured real and imaginary parts of the system response $H'(\omega)$ and $H''(\omega)$, points, and fit using the linear dispersion theory (solid line) of Eq. (3).

The cylindrical wedges are a linear system, with $H(\omega)$ defined in Eq. (3) as the complex frequency-domain system response function, $H(\omega)=H'(\omega)+iH''(\omega) = E_T(\omega,\Delta)/E_O(\omega,\Delta=0)$. $H(\omega)$ is directly measured over the range from 100 GHz to over 3 THz. Figure 3 shows the measured values of $H'(\omega)$ and $H''(\omega)$ as points for $\Delta = 100\,\mu$m. The calculated values of $H(\omega)$ from Eq. (3) are overlaid as a solid line. Similar agreement with theory is obtained for $\Delta = 200$, 500, and 1000 μm, and for the case $\theta_1 < \theta_c$.

Since the measured values of $H(\omega)$ give the complex phase change of the transmitted radiation through the wedge system, it would be theoretically possible to determine the group velocity [18] (Sec. 1.2) from $H(\omega)$ *provided the path through the system is known.* However, in representing the terahertz pulse as a superposition of phase-coherent plane waves, we are unable to measure or define the path. Definitions of path and velocity are not necessary to describe optical tunneling in this model, as the agreement between measurement and theory in Figs. 2 and 3 show. An additional, but equally important point is that $H(\omega)$ is only measurable in this experimental configuration for the wedge system as a whole and the effects of propagation in the optical tunneling barrier (gap) and in the wedges cannot be separated. The theory developed here treats the *entire* system and consequently the path taken by the radiation in the gap is not mathematically specified. Previous reports of noncausal and superluminal propagation [9] made unfounded assumptions about this path.

It is to be noted that this system is fundamentally different from the one used in recent demonstrations of superluminal propagation by Wang, Kuzmich, and Dogariu [8] in a gain medium with a well-defined optical path. For our experiment, the system transfer function has strong dispersion that changes with frequency in a nonlinear fashion. Additionally, our pulse bandwidth covering over a decade in frequency near 1 THz is over seven orders of magnitude larger than that used by Wang, Kuznich, and Dogariu with a 120 kHz bandwidth signal at a carrier frequency of 3.5×10^{14} Hz in a region of linear dispersion [8].

The theory used to fit the measurements in Fig. 2 can be demonstrated to be causal. In any causal system the real and imaginary part of $H(\omega)$ are related through the Kramers-Kronig relations [19]. To verify the causality of the theory, the real and imaginary parts of the frequency-domain response function, given by Eq. (3), were compared by numerically performing the Kramers-Kronig integral over the frequency range 0 to 20 THz. This bandwidth range is sufficient since $H(\omega)$ decreases exponentially with increasing frequency and is zero well before 20 THz. The real and imaginary components determined through the Kramers-Kronig relationships agree with the calculated and measured values of $H(\omega)$ within the experimental error. The fit shown in Fig. 3 contains no floating parameters. More precise fits are achievable by allowing for some experimental uncertainty in Δ and in the alignment of the wedge axis to that of the terahertz beam. The response function given by Eq. (3) without the correction factors γ and Φ does not satisfy the Kramers-Kronig relations.

We have measured the amplitude and phase change of picosecond terahertz electromagnetic pulses with over 3 THz bandwidth following transmission through the barrier in frustrated total internal reflection. The pulse peaks arrive earlier in time as the width of the optical tunneling gap is increased with strong reshaping due to attenuation of the high frequency components. Although similar observations [9] have led to claims of superluminal propagation of electromagnetic pulses, this is shown to be due to a description of the optical tunneling gap as an isolated object rather than integral to the entire experimental system, as well as assumptions about the path of energy propagation in the barrier. The results presented here demonstrate propagation in agreement with a causal and analytic description based on linear dispersion theory. This analytic result makes no assumptions of optical path through the gap, and contains no adjustable parameters.

The authors acknowledge Katrina McClatchey for invaluable experimental assistance, and the National Science Foundation and the Army Research Office for support of this work.

[1] R. Y. Chiao and A. M. Steinberg, in *Progress in Optics*, edited by E. Wolf (Elsevier, Amsterdam, 1997), Vol. 37, p. 345.
[2] J. Peatross, S. A. Glasgow, and M. Ware, Phys. Rev. Lett. **84**, 2370 (2000).
[3] R. L. Smith, Am. J. Phys. **38**, 978 (1970).
[4] A. Ender and G. Nimtz, Phys. Rev. E **48**, 632 (1993).
[5] R. Landauer and T. Martin, Rev. Mod. Phys. **66**, 217 (1994).
[6] T. Martin and R. Landauer, Phys. Rev. A **45**, 2611 (1992).
[7] M. Mojahedi, E. Schamiloglu, K. Agi, and K. J. Malloy, IEEE J. Quantum Electron. **36**, 418 (2000).
[8] L. J. Wang, A. Kuzmich, and A. Dogariu, Nature (London) **406**, 277 (2000).
[9] J. J. Carey, J. Zawadzka, D. A. Jaroszynski, and K. Wynne, Phys. Rev. Lett. **84**, 1431 (2000).
[10] A. M. Steinberg, P. G. Kwiat, and R. Y. Chiao, Phys. Rev. Lett. **71**, 708 (1993).
[11] P. Balcou and L. Dutriaux, Phys. Rev. Lett. **78**, 851 (1997).
[12] D. Mugnai, A. Rafagni, and R. Ruggeri, Phys. Rev. Lett. **84**, 4830 (2000).
[13] D. Mugnai, A. Ranfagni, and L. Ronchi, Phys. Lett. A **247**, 281 (1998).
[14] D. Grischkowsky, S. Keiding, M. van Exter, and Ch. Fattinger, J. Opt. Soc. Am. B **7**, 2006 (1990).
[15] P. U. Jepsen and S. R. Keiding, Opt. Lett. **20**, 807 (1995).
[16] H. K. V. Lotsch, J. Opt. Soc. Am. **58**, 551 (1968).
[17] B. R. Horowitz and T. Tamir, J. Opt. Soc. Am. **61**, 586 (1971).
[18] M. Born and E. Wolf, *Principles of Optics* (Cambridge University Press, New York, 1999).
[19] B. E. A. Saleh and M. C. Teich, *Fundamentals of Photonics* (Wiley, New York, 1991).